Journal of Environmental Chemical Engineering 8 (2020) 104467

Contents lists available at ScienceDirect

Journal of Environmental Chemical Engineering

journal homepage: www.elsevier.com/locate/jece

Investigation on adsorption behaviors of heavy metal ions (Cd^{2+}, Cr^{3+}, Hg^{2+} and Pb^{2+}) through low-cost/active manganese dioxide-modified magnetic biochar derived from palm kernel cake residue

Panya Maneechakr *, Suthep Mongkollertlop

Department of Chemistry, Faculty of Science, Rangsit University, Pathumthani 12000, Thailand

ARTICLE INFO

Editor: Zhang Xiwanga

Keywords:
MnO_2-modified magnetic biochar
Fe_3O_4
Palm kernel cake residue
Adsorption behavior
Heavy metal cation

ABSTRACT

In this study, the adsorption behaviors of heavy metal cations such as Cd^{2+}, Cr^{3+}, Pb^{2+} and Hg^{2+} were systematically investigated using active MnO_2-modified magnetic biochar derived from palm kernel cake residue. The Fe_3O_4 synthesized via co-precipitation at an optimum ratio of $FeCl_3$ to $FeCl_2$ (2 to 1) was easily coated on surface of carbonized biochar powder (CP). The adsorption performance of magnetic biochar (CP-Fe) was efficiently improved by doping with $KMnO_4$ (CP-Fe-Mn). The physicochemical properties of adsorbents were analyzed by VSM, XRD, BET, Boehm titration, FT-IR, pH_{pzc} and SEM-EDS techniques. A saturation magnetization value of CP-Fe-Mn was 20.94 emu/g, indicating to the paramagnetic properties of obtained adsorbent. A facile recovery of CP-Fe-Mn from aqueous solution after finishing adsorption process was found. The adsorption behaviors of each heavy metal ion over CP-Fe-Mn were found to be a monolayer-physisorption process, confirming by Langmuir, Dubinin-Radushkevich, Temkin, Redlich-Peterson and Toth isotherms. The maximum adsorption capacities (q_{max}) of Cd^{2+}, Cr^{3+}, Pb^{2+} and Hg^{2+} were 18.60, 19.92, 49.64 and 13.69 mg/g, respectively. A rapid adsorption with two-step of intra-particle diffusion processes followed the pseudo-second order and the Weber-Morris models, respectively. Furthermore, thermodynamic studies suggested that behavior adsorptions of heavy metals over CP-Fe-Mn were found to be spontaneous nature and endothermic process. It was expected that such a novel low-cost CP-Fe-Mn should be further applied for capable removal of several heavy metals in wastewater.

1. Introduction

As well known that the abundant existence of toxic/heavy metal such as cadmium (Cd), chromium (Cr), Mercury (Hg) and lead (Pb) in environmental wastewater become serious problems and risks for human life. In general, they are issued during production processes of metal cleaning, plating dyes, leather industry. The privation of access to safe drinkable water has been widely reported with a lot of critical issues on human health problems [1,2]. The presence of these metals, even at extremely low concentrations, lead to occurrence of carcinogen in human as identified by the US National Toxicology Program [3]. Thus, it is necessary to search some suitable direction for solving above problems. Several conventional technologies for removal of heavy metals are widely reported such as filtration membranes, ion-exchange, coagulation and co-precipitation processes [4,5]. Unfortunately, these technologies cannot be well carried out under actual field trials since they present some disadvantages, for instance, the uses of expensive equipment and chemicals are required for wastewater treatment process.

Among of all available, the utilization of activated carbon for wastewater treatment via adsorption process has been certainly regarded as a capable technique together with inexpensive [6]. Commercial activated carbon (ACC) is well known as the most common adsorbents applied to treat organic pollutants since it presents high surface area and specific functional groups. ACC also exhibits better advantages such as high capability, environmentally powerful and comparatively cheap, comparing with commercial zeolites. However, the problem of ACC application is limitation for sole removal of non-polar molecules such as phenol and iodine (I_2). In our previous work, we reported that activated carbon prepared via physical activation presented excellent adsorption performance of $Cr_2O_7^{2-}$ [7]. Also, non-polarity surface was also found for ACC based on pH_{pzc} investigation, resulting in high ability for adsorption of I_2 molecule. In the case of biochar/carbonized carbon before and after modification by $KMnO_4$, their surfaces were significantly covered

* Corresponding author.
E-mail address: panya.m@rsu.ac.th (P. Maneechakr).

https://doi.org/10.1016/j.jece.2020.104467
Received 7 July 2020; Received in revised form 4 September 2020; Accepted 6 September 2020
Available online 11 September 2020

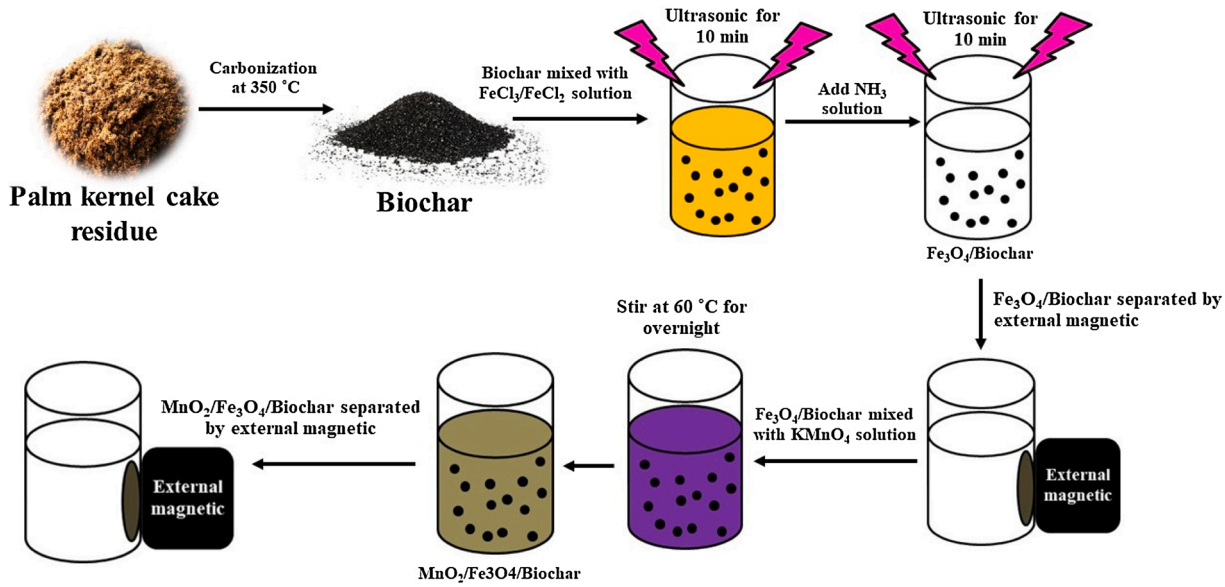

Fig. 1. Scheme illustration for preparation of CP-Fe-Mn.

by negative charge with basic properties, leading to the high performance for adsorptions of Fe^{3+}, Fe^{2+}, Ca^{2+} and Zn^{2+} [8]. However, the main problem is hindrance for eliminating and recovering the adsorbent powders from wastewater treatment system, leading to the generation of secondary pollution. In general, filtration and centrifugation processes are widely utilized to separate adsorbent powders [9]. These processes also mainly require additional time for separation and cost.

To overcome mentioned problem, a combination of adsorbent powder such activated carbon with magnetic nanoparticles should be considered and applied for metal removal process. Here, magnetic activated carbon should be easily separated by specific magnetic field. Up to now, many studies have been investigated in the topic of metal adsorption over magnetic activated carbon [10]. Wang et al. [11] found that Cr^{6+} adsorption capacity (q_e =19 mg/g) could be obtained using traditional magnetic carbon. After modification of magnetic carbon by soaking in $FeCl_3$ solution and pyrolysis, Cr^{6+} adsorption capacity was increased up to 48 mg/g. Demarchi et al. [12] succeeded in preparation of magnetic activated carbon via chemical activation using sulfuric acid for Cr^{6+} adsorption. Nejadshafiee and Islami [13] prepared a novel magnetic bio-adsorbent via 1,4-butane sultone immobilization for selective adsorption of Pb^{2+}, As^{3+} and Cd^{2+}. However, high production cost and complex technology are required for preparation of excellent magnetic adsorbent. Also, the traditional magnetic adsorbent usually has a low capacity for adsorption of heavy metal ions. Thus, it is very important to improve and modify the low-cost/green magnetic adsorbent using sustainable/cheap production process [14,15].

In this study, palm kernel cake was used as a carbon feedstock for production of biochar via carbonization process at 350 °C. Magnetic Fe_3O_4 particles were coated on biochar structure via co-precipitation using $FeCl_3$ and $FeCl_2$ under basic condition. To improve adsorption efficiency, the magnetic biochar was further modified using potassium permanganate ($KMnO_4$). The specific properties of adsorbents were characterized using SEM-EDS, Boehm titration, pH_{pzc}, VSM, XRD, FT-IR and BET. The adsorption factors such as adsorbent type, adsorbate type, ratio of adsorbent to $KMnO_4$ and pH value were optimized in details. To understand more information, the adsorption mechanisms of each metal onto adsorbent were also investigated. To the best of our knowledge, the application of MnO_2-modified magnetic biochar (CP-Fe-Mn) for selective adsorption of heavy metal ions (Cd^{2+} Cr^{3+} Hg^{2+} and Pb^{2+}) with their adsorption behaviors has not yet been reported so far. This research was expected that low-cost magnetic adsorbent should be truly applied for removal of heavy metals in environmental wastewater.

2. Experimental

2.1. Materials and reagents

Palm kernel cake was carbonized at a temperature of 350 °C under confined condition in order to obtain biochar. Then, biochar size was selected via a 400 mesh of sieve before chemical modification process. Here, the carbonized biochar powder was named as CP. The stock solutions of I_2, Fe^{2+}, Cr^{3+}, Ni^{2+}, Zn^{2+}, Cu^{2+}, Cd^{2+}, Pb^{2+}, As^{3+} and Hg^{2+} were prepared through dissolving I_2, $FeCl_2.4H_2O$, $CrCl_3.6H_2O$, $NiSO_4.6H_2O$, $ZnCl_2$, $CuSO_4.5H_2O$, $CdCl_2$, $Pb(NO_3)_2$, As_2O_3 and $HgCl_2$ in distilled water, respectively.

2.2. Adsorbent preparation

(I) For magnetic biochar (CP-Fe), 5 g CP was soaked to the mixture solution of 0.1 mol/L $FeCl_3$ (267 mL) and 0.1 mol/L $FeCl_2$ (133 mL) at ratio of Fe^{3+}: Fe^{2+} (2:1) for 10 min under ultrasonic condition. Then, 6 mol/L NH_3 solution (200 mL) was admixed to the as-prepared solution with further stirred for 10 min under ultrasonic condition. During this process, Fe_3O_4 particles were formed and coated on biochar structure via co-precipitation process between Fe^{3+} and Fe^{2+}. The adsorbent obtained from this process was named as CP-Fe. The overall reactions for magnetic Fe_3O_4 formation are provided in previous literature [16]. The CP-Fe existed in solution was easily picked using a neodymium magnet, washed exhaustively with distilled water and then dried in oven at 80 °C overnight. For pure Fe_3O_4 powder without the existence of CP was named as Fe.

(II) For MnO_2-modified magnetic biochar (CP-Fe-Mn), it was prepared via an impregnation method. In brief, 1 g of CP-Fe was soaked with 0.04 mol/L $KMnO_4$ solution at various volumes of 5−40 mL, and stirred at 60 °C for overnight. During this process, MnO_2 particles were formed and coated on CP-Fe structure. The adsorbent obtained from this process was named as CP-Fe-Mn. The CP-Fe-Mn existed in solution was easily picked using a neodymium magnet, washed with distilled water and then dried in oven at 80 °C overnight. The overall process of CP-Fe-Mn preparation is illustrated in Fig. 1. For comparison, CP-Mn was prepared using an impregnation method without the existence of Fe_3O_4. In the case of CP-Mn-Fe, CP was impregnated with $KMnO_4$ at first and followed by Fe_3O_4. The details of adsorbent characterization method using SEM-EDS, Boehm titration, pH_{pzc}, VSM, XRD, FT-IR and BET are provided in supporting information (SI) [8,17].

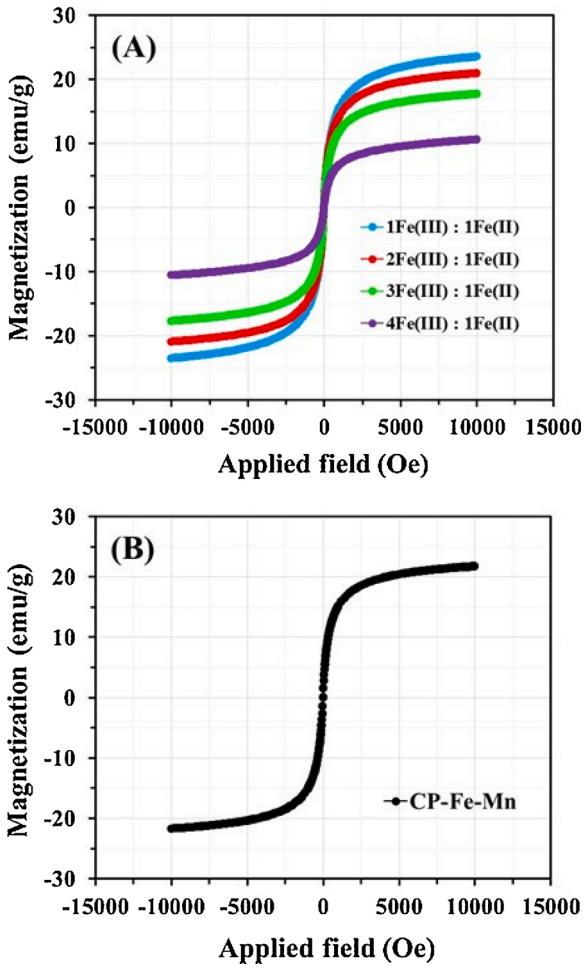

Fig. 2. Magnetization curves of (A) CP-Fe at various ratios of Fe^{3+} to Fe^{2+} and (B) CP-Fe-Mn.

2.3. Adsorbent experiment

Before investigations on adsorption behaviors/mechanisms, the adsorption capacities of the as-prepared adsorbent were primarily investigated via various factors such as adsorbent type, adsorbate type, ratio of adsorbent to $KMnO_4$ and pH value. In a typical study for adsorption procedure, the prepared adsorbent (0.2 g) was soaked in each metal ion solution (Fe^{2+}, Cr^{3+}, Ni^{2+}, Zn^{2+}, Cu^{2+}, Cd^{2+}, Pb^{2+}, As^{3+} and Hg^{2+}) at concentration of 100 mg/l with the volume of 25 mL, and stirred at 30 °C for 30 min. In the case of study on non-polar I_2 adsorption, I_2 solution at concentration of 0.05 mol/L were studied under the similar conditions with metal ion adsorption procedure. After completing the adsorption processes, the spent adsorbent was easily moved out from mixture solution by using a neodymium magnet and the remaining adsorbates existed in the achieved solutions were then analyzed. Here, the concentration amounts of Cr^{3+}, Ni^{2+}, Zn^{2+}, Cu^{2+}, Cd^{2+}, Pb^{2+}, As^{3+} and Hg^{2+} ions were quantified via external standard method using a Flame Atomic Absorption spectrometer (Thermo scientific iCE3000) For Fe^{2+} amount, it was detected by UV–vis spectrophotometer at 510 nm (Genesys 20) following a 1, 10-Phenanthroline method. The I_2 number were determined by titration method with thiosulfate ion solution. The information on adsorption isotherm, kinetic and thermodynamic procedures for are provided in SI. To determine the best-fitted model, non-linear regression and trial/error methods were applied for adsorption isotherms, kinetics and thermodynamic processes via Microsoft Excel/computer operation [19].

3. Results and discussion

3.1. Adsorption capability and behavior

Before testing on adsorption capability and behavior, the effect of mixture ratio between Fe^{3+} and Fe^{2+} for Fe_3O_4 formation on CP structure (CP-Fe) was investigated. Table S1 shows the physical properties of CP-Fe and CP-Fe-Mn. As expected, an optimum ratio of Fe^{3+} to Fe^{2+} was 2:1 based on shortest distance and time for separation process from the solution using an magnetic field. This result was in good agreement with theoretical formation of magnetic Fe_3O_4 structure. The magnetic behaviors of CP-Fe and CP-Fe-Mn were also investigated using VSM analysis. As shown in Fig. 2, the characteristic properties of magnetization curves derived from CP-Fe at virous ratios of Fe^{3+} to Fe^{2+} were classified as a soft magnetic, observing from their narrow hysteresis loops, low coercive fields and high saturation magnetization. The values of saturation magnetizations obtained from CP-Mn at Fe^{3+} to Fe^{2+} ratios of 1:1, 2:1, 3:1 and 4:1 were 23.53, 20.94, 17.71 and 10.56 emu/g, respectively, suggesting to typical ferrimagnetic or ferrite properties. As observed, the magnetic properties of CP-Fe were decreased to some extent with the increasing of Fe^{3+} adding amount. This indicates that excess amount of $FeCl_3$ adding obstructed the formation of Fe_3O_4 on CP surface. It should be noted that superparamagnetic properties were occurred at saturation magnetization value of ≥60 emu/g [20]. However, this saturation magnetization value could be possibly reduced in the presence of nonmagnetic materials such as activated carbon. For CP-Fe-Mn, ferrimagnetic or ferrite properties were presented with a saturation magnetization value of 21.76 emu/g. The magnetization values of the as-prepared samples were acceptable which could be easily separated easily from aqueous solution using a neodymium magnet. From these results, CP-Fe at Fe^{3+} to Fe^{2+} ratio of 2:1 was chosen for next studies.

Fig. S1 presents the adsorption abilities of non-polar I_2 molecule and Fe^{2+}ion by using various adsorbents. It is found that CP before and after modification exhibited lower I_2 adsorption abilities than ACC. In contrast, lower Fe^{2+} adsorption ability was found for ACC when compared with CP before and after modification, suggesting to the low polarity of ACC. Comparing on CP, CP-Fe and CP-Mn, one can see that CP-Mn exhibited highest capacity (q_e =73.93 mg/g) for Fe^{2+} adsorption, indicating that $KMnO_4$ activation created the significant formation of functional oxygens such carbonyl/carboxylic groups as including of MnO_2 (-C-C−OH + $KMnO_4$ → + -C−COOH + -C-C = O + MnO_2) on CP surface for improving the adsorption of metal cation [15]. As well known that Lewis acid properties of metal cations could be easily adsorbed onto adsorbent surface containing large amounts of oxygenated compounds such as carbonyl groups with the presence of lone pairs of electrons (Lewis base properties) over electrostatic forces, generating the covalent bonds [21]. Unfortunately, very low capacity for Fe^{2+} adsorption was found for CP-Fe, resulting from the presence of Fe_3O_4 with high amount. This also revealed that Fe_3O_4 coated on CP could well help for separation process but it did not improve the efficiency for metal cation adsorption. To solve above problem, CP-Fe was modified by $KMnO_4$ activation (CP-Fe-Mn). As expected, the Fe^{2+} adsorption capability was well improved with addition in the ratio of CP-Fe: Mn from 1:5 (q_e =17.85 mg/g) to 1:25 (q_e =46.38 mg/g). It should be noted that too high $KMnO_4$ loading amount such as CP-Fe to Mn ratios of 1:30 and 1:40 could lead to the reduction of Fe^{2+} adsorption ability. This phenomenon might be attributed to pore blockade which occurred from the existence of MnO_2 with high amount on outer surface of CP-Fe, leading to the diffusion resistance of adsorbate. In addition, the CP-Fe-Mn in each ratio had higher capacities for Fe^{2+} adsorption than CP-Fe, except for CP-Mn. Therefore, CP-Fe-Mn at a ratio of 1:25 was selected for further studies.

Fig. S2 presents the Fe^{2+} adsorption ability of each adsorbent. The efficiency of as-prepared adsorbent for Fe^{2+} removal based on q_e value was in the order of CP-Mn > CP-Fe-Mn > Fe-Mn > CP-Mn-Fe > CP > CP-Fe > Fe. Here, all adsorbents oxidized by $KMnO_4$ exhibited excellent

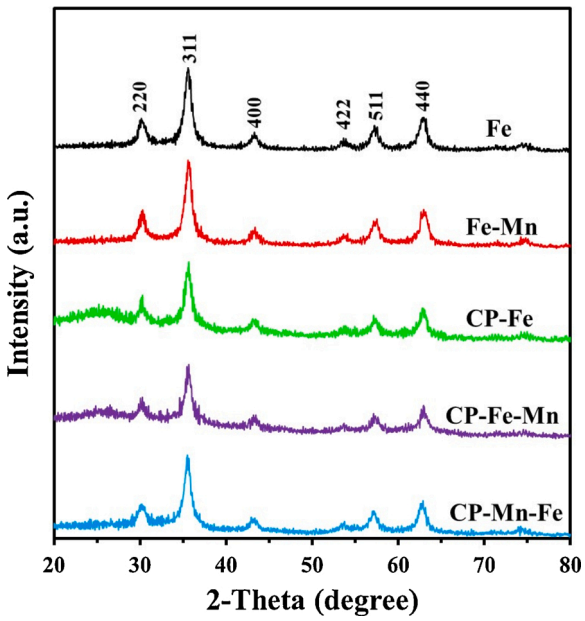

Fig. 3. XRD patterns of as-prepared adsorbents.

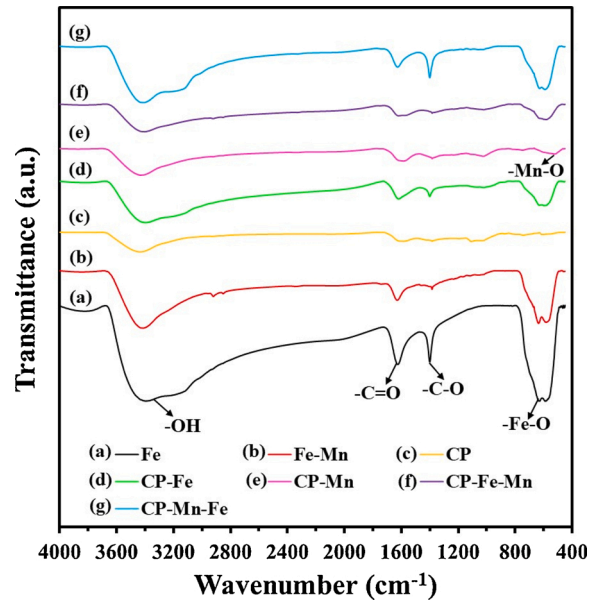

Fig. 4. FT-IR spectra of as-prepared adsorbents.

ability for Fe^{2+} adsorption. This could be attributed to the existence of two oxygen atoms of MnO_2 coated on adsorbent surface, promoting the Fe^{2+} adsorption efficiency. The lowest ability for Fe^{2+} adsorption was found for Fe (q_e =2.34 mg/g). Interestingly, the Fe^{2+} adsorption capacity was increased up to 20 times when Fe was modified by $KMnO_4$ (Fe-Mn). Comparing between CP-Fe-Mn with CP-Mn-Fe, one can see that CP-Mn-Fe exhibited lower efficiency for Fe^{2+} adsorption than CP-Fe-Mn even $KMnO_4$ loading amount on them was the similar. This difference suggests that surface of CP-Fe-Mn was mainly covered by MnO_2 while CP-Mn-Fe would be Fe_3O_4. It could be confirmed that the existence of MnO_2 on adsorbent surface was greatly required for efficient adsorption of metal cation. Fig. S3 presents the adsorption capacities of Cr^{3+}, Ni^{2+}, Zn^{2+}, Cu^{2+}, Cd^{2+}, Pb^{2+}, As^{3+} and Hg^{2+}. The CP-Fe-Mn exhibited the excellent adsorption performance of all types of heavy metals, especially for Pb^{2+} (q_e =49.73 mg/g). It should be noted that four heavy metal ions such as Cd^{2+}, Cr^{3+}, Hg^{2+} and Pb^{2+} were selected for further investigation on their adsorption behaviors via virous effects such as pH, adsorption equilibriums, adsorption kinetics and adsorption thermodynamics using CP-Fe-Mn since they exhibited high adsorption capacities. From these results, the CP-Fe-Mn could be possibly applied for selective removal of several metals from wastewater in environment and also easily separated by using a neodymium magnet.

3.2. Characterization of adsorbent

To confirm magnetic structure, the XRD patterns of as-prepared magnetic adsorbents are presents in Fig. 3. All samples clearly appeared the diffraction peaks at 30, 35, 43, 54, 57 and 63°, which corresponded to (220), (311), (400), (422), (511) and (440) of Fe_3O_4 crystal structure [22]. In general, the diffraction peaks at 29, 38 and 40° should be appeared for XRD pattern of MnO_2 [8]. However, in this study, the diffraction peaks of MnO_2 did not found, suggesting that it might be overlapped at the same position with Fe_3O_4 structure were about 30, 36 and 43° [15]. The broad peaks at 2θ around 20−30° were appeared for CP, CP-Fe-Mn and CP-Mn-Fe, according to amorphous carbon structure [18,23]. In addition, weaker intensity peaks of Fe_3O_4 was found for CP-Fe-Mn when compared with CP-Mn-Fe, resulting from the covering by MnO_2. Fig. 4 presents the FT-IR spectra of as-prepared magnetic adsorbents. All samples exhibited the vibration peaks at wavenumbers of 3600−3000, 1630 and 1030 cm^{-1}, which could be described on oxygen groups such as −OH, -C = O and -C-O, respectively [24]. For magnetic adsorbents such as Fe, Fe-Mn, CP-Fe, CP-Fe-Mn and CP-Mn-Fe, the strong vibration peak was found at around 560 cm^{-1}, associating to Fe-O functional group [25]. For comparison, Fe sample presented highest intensity peak of Fe-O, probably due to high purity of Fe_3O_4. Here, as expected, higher intensity peak of Fe-O was observed for CP-Mn-Fe when compared with CP-Fe-Mn. These data were in good consent with XRD results in Fig. 3. The weak vibration peak at around 500 cm^{-1} was found for CP-Mn, which could be attributed to Mn-O functional group of MnO_2. It should be noted that the wavenumber of MnO_2 absorption peak was close to Fe_3O_4 absorption peak, leading to the overlapping in each other as obtained results of FT-IR spectra in Fig. 4.

The morphologies of the as-prepared magnetic adsorbents and the presence of Fe and Mn elements were shown in Fig. 5. As observed, the surface morphologies of each adsorbent were craggy and uneven, resulting from the covering of Fe_3O_4 and MnO_2 particles. In the case of CP without modification of Fe_3O_4 and MnO_2, the surface morphology had smooth/flat (Fig. S5). The amounts of various elements such as C, O, Fe and Mn were provided in Table S2. As shown in Fig. 5, the EDS results also confirm that Fe and Mn elements were existed and well distributed on the surface of support. Table 1 and Fig. S4 show the surface charges of CP-Fe-Mn. Here, pH_{pzc} value was applied to determine the surface charge properties of adsorbent. As achieved, the pH_{pzc} value of CP-Fe-Mn was >8, suggesting that its surface was dominated by negative charge which occurred from the existence of MnO_2 and C═O groups on the surface. Meanwhile, the all adsorbates used in this study had positive charge, leading to the excellent efficiency for adsorption process. The acidity and basicity of CP, CP-Fe and CP-Fe-Mn are shown in Table 2. It is found that the amounts of carboxylic, lactone and/or phenolic groups on CP surface were significantly decreased after coating by Fe_3O_4. Interestingly, the basic amount of CP was favorable enhanced from 2.26 to 4.16 and 6.60 meq/g when compared with CP-Fe and CP-Fe-Mn, respectively. This should be described on the formation of Fe_3O_4 or MnO_2 which occurred from reaction with HCl, resulting in the increase of basic amount on CP-Fe and CP-Fe-Mn. Here, the carboxylic groups on CP-Fe-Mn were clearly increased to be 0.15 meq/g when compared with CP-Fe (0.04 meq/g), resulting from oxidation reaction at −OH regions. In addition, the surface area of CP was 6.4 m^2/g (Table 2). After Fe_3O_4 or MnO_2 was coated onto CP structure, its surface area was further increased about 14 times. This indicates that the metal adsorption efficiency was very well improved. As obtained result, it was different from

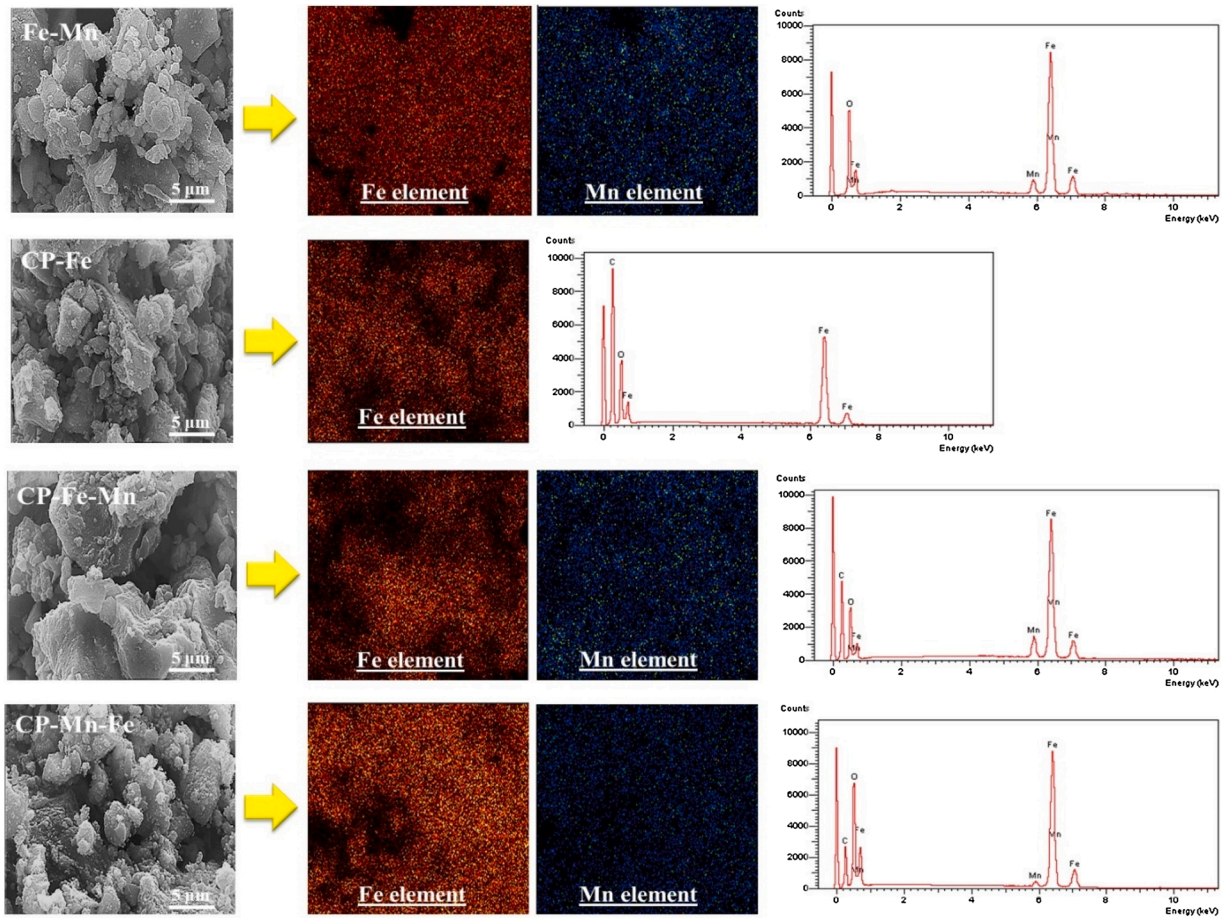

Fig. 5. SEM-EDS images of as-prepared adsorbents.

Table 1
Surface charges of CP-Fe-Mn in each metal solution.

	pH_{pzc}	pH in solution			
	NaCl	Cd^{2+}	Cr^{3+}	Pb^{2+}	Hg^{2+}
No adsorbent	6.89	5.60	3.14	4.93	4.49
CP-Fe-Mn	8.62	7.07	4.30	7.93	7.93

those reported ones, in which the surface area was always reduced by metal addition due to the pore blocking [25]. It is plausible that the contribution of Fe_3O_4 and MnO_2 particles generated new extra- roughness surface area and small pore on CP structure.

3.3. *Effect of pH on Cd^{2+}, Cr^{3+}, Pb^{2+} and Hg^{2+} adsorptions*

The effect of pH value adjusting for Cd^{2+}, Cr^{3+}, Pb^{2+} and Hg^{2+} adsorptions using CP-Fe-Mn are shown in Fig. 6. One can clearly see that at low pH value in metal solution, high amount of H_3O^+ ion was generally existed and could be reacted with MnO_2 (basicity properties), leading to the inability of CP-Fe-Mn for metal adsorption. It seems that the ability of metal adsorption was enhanced to some extent with an increase in pH value of metal solution. In the case of too high pH value in aqueous solution, Cr^{3+} and Hg^{2+} (at pH value of > 4) with Cd^{2+} and Pb^{2+} (at pH value of > 7) ions could initially slit with −OH to form the precipitates of metal hydroxides. Therefore, high capacities for Cd^{2+}, Cr^{3+}, Pb^{2+} and Hg^{2+} adsorptions at high pH value did not result from using CP-Fe-Mn. Meanwhile, the magnetic properties with separation efficiency of CP-Fe-Mn might be easily destroyed from the reaction between Fe_3O_4 with H_3O^+ at low or high pH value. Based on above result, it suggests that the adsorption process of metal cations using CP-Fe-Mn could be enough performed at neutral pH controlled under environmental conditions.

The effects of metal desorption and regeneration/reusability did not investigate. Here, it may be exactly forecasted based on our previous works that the metal desorption ability was easily achieved by washing with nitric acid solution [8]. In the same way, Fe_3O_4 and MnO_2 coated on CP surface could be also leached during washing with nitric acid solution, leading to ineffective reusability. However, considering on production cost of CP-Fe-Mn in Thailand zone, a total price was about 10 USD/kg consisting of biochar (0.6 USD/kg), grinding charge (0.6 USD /kg), $KMnO_4$ reagent (4.2 USD), Fe_3O_4 coating (3.3 USD), This indicates that as-prepared adsorbent was much lower-priced when compared with

Table 2
Characteristic properties of each adsorbents.

Adsorbent	BET surface Area (m^2/g)	Amount of functional groups (meq/g)					
		Carboxylic	Lactone	Phenolic	Acidity	Basicity	Total acidity and basicity
CP	6.4078	0.0745	0.0359	4.0212	4.1316	2.2612	6.3928
CP-Fe	90.1873	0.0400	0.0202	2.0115	2.0717	4.1561	6.2278
CP-Fe-Mn	89.3853	0.1458	0.0355	0.3256	0.3769	6.5961	7.1030

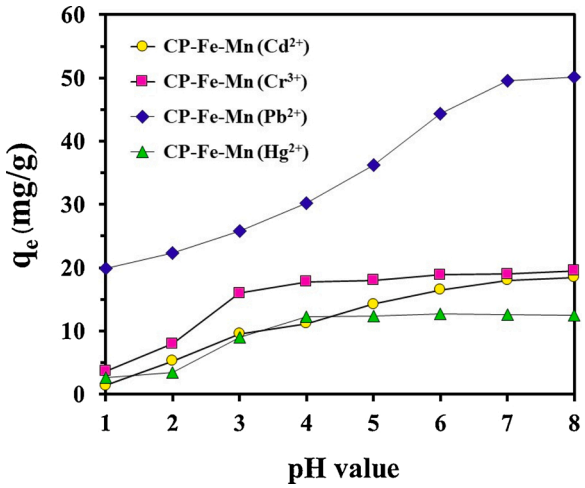

Fig. 6. Effect of pH value on the adsorption of Cd^{2+}, Cr^{3+}, Pb^{2+} and Hg^{2+} by CP-Fe-Mn.

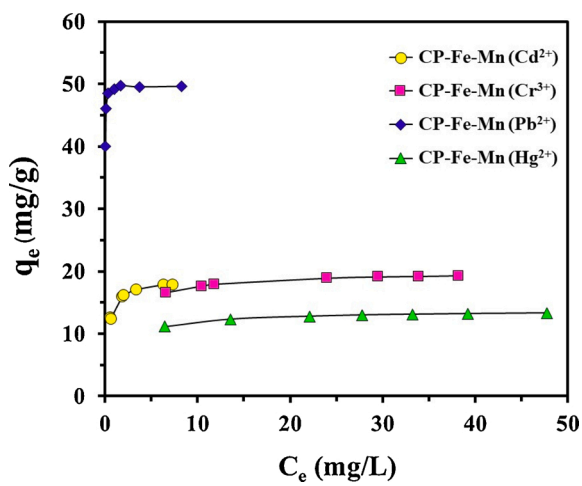

Fig. 7. Equilibrium adsorption of Cd^{2+}, Cr^{3+}, Pb^{2+} and Hg^{2+} by CP-Fe-Mn.

commercial activated carbon (132 USD/kg). Meanwhile, CP-Fe-Mn also obviously presented higher metal adsorption efficiency than commercial activated carbon. Therefore, this is not necessary to be considered for regeneration process.

3.4. Adsorption equilibrium

In this study, mathematical six model such as Langmuir, Freundlich, Dubinin-Radushkevich, Temkin, Redlich-Peterson and Toth isotherms were used to describe the adsorption behavior and interaction of Cd^{2+}, Cr^{3+}, Pb^{2+} and Hg^{2+} onto CP-Fe-Mn. The details in each isotherm and their equations are also provided in SI [26–29]. Fig. 7 and Table 3 present the results of equilibrium adsorption isotherms of Cd^{2+}, Cr^{3+}, Pb^{2+} and Hg^{2+} using CP-Fe-Mn which calculated from non-linear method. One can see that Langmuir model was very fitted based on R^2 value close to 1, comparing to Freundlich model. This indicates that adsorption behaviors of Cd^{2+}, Cr^{3+}, Pb^{2+} and Hg^{2+} were monolayer adsorption process over electrostatic forces, generating the covalent bonds. This behavior might possible to be chemical/physical adsorptions due to monolayer adsorption mechanism. Here, the q_{max} of Cd^{2+}, Cr^{3+}, Pb^{2+} and Hg^{2+} adsorptions using CP-Fe-Mn were found be 18.60, 19.92, 49.64 and 13.69 mg/g, respectively. Meanwhile, the metal adsorption capabilities were in the order of $Pb^{2+} > Cr^{3+} > Cd^{2+} > Hg^{2+}$. In the case of Temkin model, it is found that R^2 values of Cd^{2+}, Cr^{3+}, Pb^{2+} and Hg^{2+} adsorptions were close to 1, indicating that all parameters calculated in this model were acceptable. It should be noted that a maximum *A* value was found for Pb^{2+} ion, suggesting to strongest energy for equilibrium adsorption of Pb^{2+} onto CP-Fe-Mn surface. To know more details on adsorption process, *E* value calculated from Dubinin-Radushkevich model was also considered. As known that the range of *E* value at 8−16 kJ/mol was referred to the chemisorption behavior [30], relating to adsorption behavior of CP-Fe-Mn with Pb^{2+} ion. The *E* values of Cd^{2+}, Cr^{3+} and Hg^{2+} adsorptions were < 8 kJ/mol, suggesting to physisorption behavior. This phenomenon might be a reason that Pb^{2+} adsorption ability was much higher when compared the other metals. Interestingly, q_s value from Dubinin-Radushkevich model was approach to q_{max} value from Langmuir model, suggesting to high propriety of applied model. The assumption of Langmuir model provided in this study was also supported with parameters such as g constant, Th and their R^2 under Toth or Redlich-Peterson isotherm, verifying to monolayer adsorption mechanism. These results were in the good agreement with Langmuir model. Based on above results, CP-Fe-Mn had excellent potential for selective adsorption of heavy

Table 3
Isotherms and their parameters obtained from equilibrium adsorption of Cd^{2+}, Cr^{3+}, Pb^{2+} and Hg^{2+} by CP-Fe-Mn.

Adsorbent	Metal ions	Langmuir parameters			Freundlich parameters		
		q_{max} (mg/g)	K (L/mg)	R^2	1/n	K_F	R^2
CP-Fe-Mn	Cd^{2+}	18.60	3.45	0.9977	0.14	14.06	0.9240
	Cr^{3+}	19.92	0.74	0.9996	0.08	14.53	0.9656
	Pb^{2+}	49.64	135.20	0.9986	0.03	48.06	0.7158
	Hg^{2+}	13.69	0.67	0.9992	0.09	9.69	0.9479

Adsorbent	Metal ions	Temkin parameters			Dubinin-Radushkevich parameters			
		b	A (L/mol)	R^2	q_s (mg/g)	B (mol^2/J^2)	*E* (kJ/mol)	R^2
CP-Fe-Mn	Cd^{2+}	1120.15	574.47	0.9506	18.00	9.93E-08	3.17	0.8532
	Cr^{3+}	1673.35	12791.12	0.9720	19.14	1.33E-06	0.87	0.9493
	Pb^{2+}	1622.25	4.84E+13	0.9984	51.39	5.10E-09	14.00	0.8317
	Hg^{2+}	2310.02	5961.90	0.9590	13.06	1.09E-06	0.96	0.8852

Adsorbent	Metal ions	Redlich-Peterson parameters				Toth parameters			
		A	B	g	R^2	q_e^{∞}	K_{Th}	Th	R^2
CP-Fe-Mn	Cd^{2+}	67.64	3.70	0.99	0.9981	18.82	0.28	0.92	0.9980
	Cr^{3+}	51.90	3.32	0.94	0.9818	20.03	1.14	0.94	1.0000
	Pb^{2+}	6830.43	137.67	1.00	0.9987	49.70	0.01	0.95	0.9990
	Hg^{2+}	9.84	0.74	0.99	0.9997	13.81	1.17	0.91	1.0000

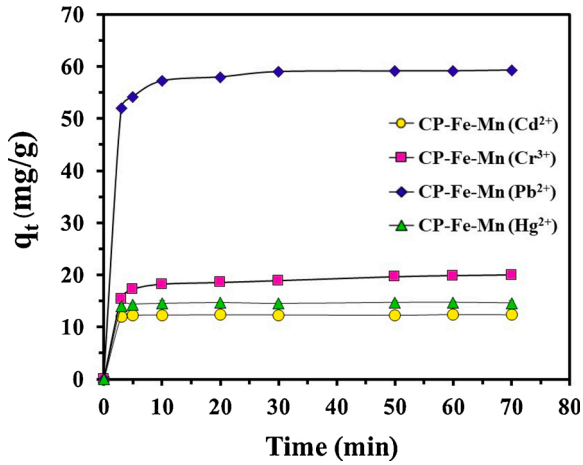

Fig. 8. Effect of contact time for the adsorption of Cd^{2+}, Cr^{3+}, Pb^{2+} and Hg^{2+} by CP-Fe-Mn.

metal, especially for Pb^{2+} ion since highest values of q_{max}, q_s and q_e^{∞} were certainly obtained in this study.

3.5. Adsorption kinetic

Fig. 8 presents the adsorption capabilities of Cd^{2+}, Cr^{3+}, Pb^{2+} and Hg^{2+} at different contact times using CP-Fe-Mn. As seen, a speedy adsorption of each metal was firstly commenced at contact time of 3 min. Thereafter, the similar trends in each metal ions were gently enhanced which was close to equilibrium at contact time of 30 min. This spectacle may be described to the abundant existence of adsorption sites [31]. The specific factors obtained from adsorption kinetic model are presented in Table 4 . The details of adsorption kinetic and their equations are also provided in SI [32,33]. The adsorption kinetics of Cd^{2+}, Cr^{3+}, Pb^{2+} and Hg^{2+} onto CP-Fe-Mn surface were observed to be ruled over pseudo second-order (based on $R^2 > 0.99$), suggesting a rapid adsorption behavior. In addition, the kinetic model in this study had high accuracy based on approximation of q_e obtained from calculation and experiment. To derive more details for the adsorption behavior, Weber-Morris model was used to define the influence of intra-particle diffusion [34], and the result is presented in Fig. 9.

The plots exhibited multi-linearity, suggesting that 2 steps of intra-particle diffusion were emerged from the adsorption procedure. From this experiment, the adsorption processes of Cd^{2+}, Cr^{3+}, Pb^{2+} and Hg^{2+} onto CP-Fe-Mn were complex with boundary layer diffusion process. As observed, the initial sharper portion was described to the instantaneous adsorption or exterior surface adsorption. The next portion was the last adsorption phase which intra-particle diffusion began to decelerate due to the low concentration amount of adsorbate in the aqueous solutions [35].

3.6. Adsorption thermodynamic

Fig. 10 presents the effect of adsorption of Cd^{2+}, Cr^{3+}, Pb^{2+} and Hg^{2+} at different temperatures using CP-Fe-Mn. It is found that the adsorption capabilities of Cd^{2+}, Cr^{3+}, Pb^{2+} and Hg^{2+} using CP-Fe-Mn were increased to some extent with the increase in adsorption temperature. This phenomenon was generally attributed to the endothermic adsorption behaviour. Also, the increasing of temperature reduced the viscosity of solution, promoting a diffusion rate of ion athwart the exterior boundary layer as well as the interior porous of the CP-Fe-Mn structure. To assess the effect of adsorption temperature of Cd^{2+}, Cr^{3+}, Pb^{2+} and Hg^{2+}, the thermodynamic process was studied. The details of adsorption thermodynamic and their equations are also provided in SI [36]. The factors obtained from thermodynamic study are presented in Table 5. As expected, the negative values of Gibbs standard free energy (ΔG) was obtained for all metal ions while ΔG value was significantly reduced

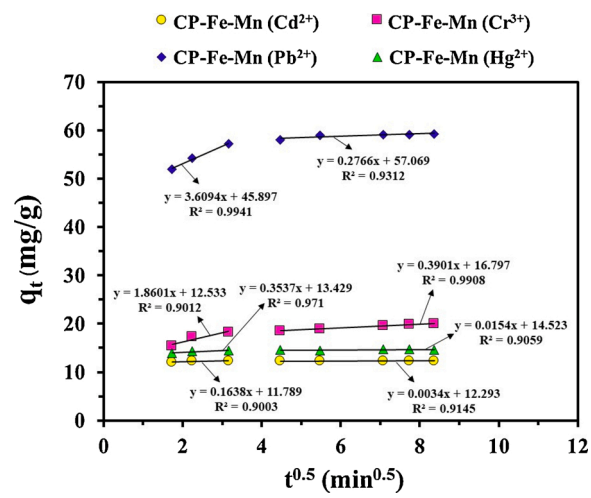

Fig. 9. Intra-particle diffusion plot for adsorption of Cd^{2+}, Cr^{3+}, Pb^{2+} and Hg^{2+} by CP-Fe-Mn.

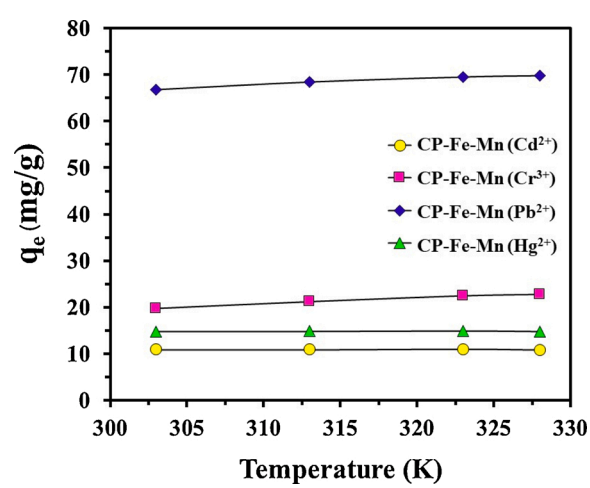

Fig. 10. Effect of temperature for the adsorption of Cd^{2+}, Cr^{3+}, Pb^{2+} and Hg^{2+} by CP-Fe-Mn.

Table 4
Pseudo-first order and pseudo-second order kinetic model parameters obtained from effect of contact time for the adsorption of Cd^{2+}, Cr^{3+}, Pb^{2+} and Hg^{2+} by CP-Fe-Mn.

Adsorbent	Metal ions	$q_{e\ exp}$ (mg/g)	Pseudo-first-order			Pseudo-second-order		
			$q_{e\ cal}$	k_1	R^2	$q_{e\ cal}$	k_2	R^2
CP-Fe-Mn	Cd^{2+}	12.45	0.16	0.01	0.4554	12.37	0.70	1.0000
	Cr^{3+}	20.00	88.10	0.13	0.7612	20.23	0.04	0.9997
	Pb^{2+}	59.30	6.15	0.07	0.9284	58.41	0.13	0.9994
	Hg^{2+}	14.71	1.00	0.07	0.6588	14.67	0.53	1.0000

Table 5
Thermodynamic parameters obtained from effect of temperature for the adsorption of Cd^{2+}, Cr^{3+}, Pb^{2+} and Hg^{2+} by CP-Fe-Mn.

Adsorbent	Metal ions	ΔH/(kJ/mol)	ΔS/(J/mol K	ΔG/(kJ/mol)				R^2
				303 K	313 K	323 K	328 K	
CP-Fe-Mn	Cd^{2+}	34.96	149.58	−10.19	−11.18	−12.13	−12.86	0.9915
	Cr^{3+}	51.64	184.00	−4.05	−5.60	−7.13	−7.91	0.9995
	Pb^{2+}	56.54	211.05	−7.35	−8.85	−10.63	−11.57	0.9950
	Hg^{2+}	4.87	54.34	−11.34	−11.49	−11.65	−11.70	0.9984

Table 6
The comparison of adsorption abilities of each metal cation using CP-Fe-Mn with other adsorbents.

Adsorbent	q_e of Cd^{2+} (mg/g)	q_e of Pb^{2+} (mg/g)	q_e of Hg^{2+} (mg/g)	q_e of Cr^{3+} (mg/g)	Ref.
Ca-MBC	10.11	–	–	–	[39]
MBC	14.96	25.29	–	–	[40]
MBC	11.04	26.08	–	–	[41]
MECBC	–	40.57	–	–	[42]
MCW-2	–	41.19		–	[43]
Fe_3O_4-GS	27.83	27.95	23.03		[44]
Exhausted coffee waste	–	–	31.75	–	[45]
CM-BT	–	–	–	20.90	[46]
Na^+-SiO_2 spheres	–	–	–	33.18	[47]
CP-Fe-Mn	18.60	49.64	13.69	22.38	This work

when the adsorption temperature was increased from 303 to 328 K, attributing a spontaneous nature for Cd^{2+}, Cr^{3+}, Pb^{2+} and Hg^{2+} adsorption behaviours using CP-Fe-Mn. Here, the altering in free energy for chemisorption the range was in between −80 to −400 kJ/mol while physisorption process was in the range between −20 to 0 kJ/mol. This indicates that range of ΔG values (−4.05 to −12.86 kJ/mol) obtained from Cd^{2+}, Cr^{3+}, Pb^{2+} and Hg^{2+} adsorptions using CP-Fe-Mn were indicated to be physisorption process [37]. The endothermic nature of Cd^{2+}, Cr^{3+}, Pb^{2+} and Hg^{2+} adsorptions with irreversible/randomness processes were proved since standard enthalpy (ΔH) and standard entropy (ΔS) factors had positive values [38]. In addition, based on $\Delta H < 100$ kJ/mol, physisorption behavior was also proved, suggesting in well agreement with Dubinin-Radushkevich isotherm result. As shown in Table 6, CP-Fe-Mn exhibited good results for adsorption abilities in each metal cation when compared with other adsorbents previously reported in several literatures. From these results, CP-Fe-Mn could be expected to be further applied as a promising low-cost/efficient adsorbent for selective removal of heavy metals in environmental wastewater.

4. Conclusions

The CP-Fe-Mn was easily prepared via cheap process, and successfully utilized for facile adsorption of Cd^{2+}, Cr^{3+}, Pb^{2+} and Hg^{2+} ions from aqueous solution. The spent CP-Fe-Mn was easy to be recovered from aqueous solution by using a neodymium magnet, comparing to traditional activated carbon. The contribution of carboxylic group and MnO_2 on CP surface as well as its basicity properties well promoted the adsorption efficiency, confirming by FT-IR Boehm titration and pH_{pzc} results. ACC was found to be only favored for I_2 molecular. For adsorption behaviors of Cd^{2+}, Cr^{3+}, Pb^{2+} and Hg^{2+} onto CP-Fe-Mn surface, they were well fitted based on R^2 values close to 1 for non-linear isotherm/kinetic models. The highest q_{max} derived from Langmuir isotherm for Cd^{2+}, Cr^{3+}, Pb^{2+} and Hg^{2+} ions using CP-Fe-Mn were 18.60, 19.92, 49.64 and 13.69 mg/g, respectively. The 2 step intraparticle diffusions of Cd^{2+}, Cr^{3+}, Pb^{2+} and Hg^{2+} ions onto CP-Fe-Mn were also found. Moreover, the thermodynamic study indicated that the adsorption behavior was physisorption and endothermic procedures.

CRediT authorship contribution statement

Panya Maneechakr: Conceptualization, Writing - original draft, Writing - review & editing. **Suthep Mongkollertlop:** Conceptualization, Methodology.

Declaration of Competing Interest

The authors declare that they have no known competing financial interests or personal relationships that could have appeared to influence the work reported in this paper.

Acknowledgements

The authors would like to gratefully appreciate Research Institute of Rangsit University, and Department of Chemistry, Faculty of Science, Rangsit University, Thailand for research fund and supporting all chemicals, equipment and instruments

Appendix A. Supplementary data

Supplementary material related to this article can be found, in the online version, at doi:https://doi.org/10.1016/j.jece.2020.104467.

References

[1] Q. Shi, A. Terracciano, Y. Zhao, C. Wei, C. Christodoulatos, X. Meng, Evaluation of metal oxides and activated carbon for lead removal: kinetics, isotherms, column tests, and the role of co-existing ions, Sci. Total Environ. 648 (2019) 176–183.
[2] W. Liu, J. Zhang, C. Zhang, Y. Wang, Y. Li, Adsorptive removal of Cr (VI) by Fe-modified activated carbon prepared from *Trapa natans* husk, Chem. Eng. J. 162 (2010) 677–684.
[3] S. Hokkanen, A. Bhatnagar, E. Repo, S. Lou, M. Sillanpää, Calcium hydroxyapatite microfibrillated cellulose composite as a potential adsorbent for the removal of Cr (VI) from aqueous solution, Chem. Eng. J. 283 (2016) 445–452.
[4] J. Cui, C. Jing, D. Che, J. Zhang, S. Duan, Groundwater arsenic removal by coagulation using ferric (III) sulfate and polyferric sulfate: a comparative and mechanistic study, J. Environ. Sci. 32 (2015) 42–53.
[5] Y. Huang, D. Wu, X. Wang, W. Huang, D. Lawless, X. Feng, Removal of heavy metals from water using polyvinylamine by polymer-enhanced ultrafiltration and flocculation, Sep. Purif. Technol. 158 (2016) 124–136.
[6] H.D. Choi, W.S. Jung, J.M. Cho, B.G. Ryu, J.S. Yang, K. Baek, Adsorption of Cr(VI) onto cationic surfactant-modified activated carbon, J. Hazard. Mater. 166 (2009) 642–646.
[7] P. Maneechakr, S. Karnjanakom, Adsorption behaviour of Fe(II) and Cr(VI) on activated carbon: surface chemistry, isotherm, kinetic and thermodynamic studies, J. Chem. Thermodyn. 106 (2017) 104–112.
[8] P. Maneechakr, S. Karnjanakom, Environmental surface chemistries and adsorption behaviors of metal cations (Fe^{3+}, Fe^{2+}, Ca^{2+} and Zn^{2+}) on manganese dioxide-modified green biochar, RSC Adv. 9 (2019) 24074–24086.
[9] J. Niu, P. Ding, X. Jia, G. Hu, Z. Li, Study of the properties and mechanism of deep reduction and efficient adsorption of Cr(VI) by low-cost Fe_3O_4-modified ceramsite, Sci. Total Environ. 688 (2019) 994–1004.
[10] Y. Shan, W. Yang, Y. Li, Y. Liu, J. Pan, Preparation of microwave-activated magnetic bio-char adsorbent and study on removal of elemental mercury from flue gas, Sci. Total Environ. 697 (2019), 134049.
[11] F. Wang, L.Y. Liu, F. Liu, L.G. Wang, T. Ouyang, C.T. Chang, Facile one-step synthesis of magnetically modified biochar with enhanced removal capacity for hexavalent chromium from aqueous solution, Taiwan Inst. Chem. Eng. 81 (2017) 414–418.
[12] C.A. Demarchi, B.S. Michel, N. Nedelko, A. Ślawska-Waniewska, P. Dłużewski, A. Kaleta, R. Minikayev, T. Strachowski, L. Lipińska, J.D. Magro, C.A. Rodrigues, Preparation, characterization, and application of magnetic activated carbon from termite feces for the adsorption of Cr(VI) from aqueous solutions, Powder Technol. 354 (2019) 432–441.

[13] V. Nejadshafiee, M.R. Islami, Adsorption capacity of heavy metal ions using sultone-modified magnetic activated carbon as a bio-adsorbent, Mater. Sci. Eng., C 101 (2019) 42–52.
[14] M.H. Fatehi, J. Shayegan, M. Zabihi, I. Goodarznia, Functionalized magnetic nanoparticles supported on activated carbon for adsorption of Pb(II) and Cr(VI) ions from saline solutions, J. Environ. Chem. Eng. 5 (2017) 1754–1762.
[15] N.C. Feng, W. Fan, M.L. Zhu, X.Y. Guo, Adsorption of Cd^{2+} in aqueous solutions using $KMnO_4$-modified activated carbon derived from *Astragalus* residue, Trans. Nonferrous Met. Soc. China 28 (2018) 794–801.
[16] M.Y. Badi, A. Azari, H. Pasalari, A. Esrafili, M. Farzadkia, Modification of activated carbon with magnetic Fe_3O_4 nanoparticle composite for removal of ceftriaxone from aquatic solutions, J. Mol. Liq. 261 (2018) 146–154.
[17] R.B. Fidel, D.A. Laird, M.L. Thompson, Evaluation of modified boehm titration methods for use with biochars, J. Environ. Qual. 42 (2013) 1771–1778.
[18] P. Maneechakr, S. Karnjanakom, The essential role of Fe(III) ion removal over efficient/low-cost activated carbon: surface chemistry and adsorption behaviour, Res. Chem. Intermed. 45 (2019) 4583–4605.
[19] Y.S. Ho, Isotherms for the sorption of lead onto peat: comparison of linear and non-linear methods, Pol. J. Environ. Stud. 15 (2016) 81–86.
[20] R.S. Juang, Y.C. Yei, C.S. Liao, K.S. Lin, H.C. Lu, S.F. Wang, A.C. Sun, Synthesis of magnetic Fe_3O_4/activated carbon nanocomposites with high surface area as recoverable adsorbents, Taiwan Inst. Chem. Eng. 90 (2018) 51–60.
[21] W. Shen, Z. Li, Y. Liu, Surface chemical functional groups modification of porous carbon, Recent Patents on Chem. Eng. 1 (2008) 27–40.
[22] S. Liang, S. Shi, H. Zhang, J. Qiu, W. Yu, M. Li, Q. Gan, W. Yu, K. Xiao, B. Liu, J. Hu, H. Hou, J. Yang, One-pot solvothermal synthesis of magnetic biochar from waste biomass: formation mechanism and efficient adsorption of Cr(VI) in an aqueous solution, Sci. Total Environ. 695 (2019), 133886.
[23] S. Karnjanakom, P. Maneechakr, Designs of linear-quadratic regression models for facile conversion of carbohydrate into high value (5-(ethoxymethyl)furan-2-carboxaldehyde) fuel chemical, Energy Convers. Manage. 196 (2019) 410–417.
[24] H. Zhou, X. Zhu, B. Chen, Magnetic biochar supported α-MnO_2 nanorod for adsorption enhanced degradation of 4-chlorophenol via activation of peroxydisulfate, Sci. Total Environ. 724 (2020), 138278.
[25] C. Sun, T. Chen, Q. Huang, J. Wang, S. Lu, J. Yan, Enhanced adsorption for Pb(II) and Cd(II) of magnetic rice husk biochar by $KMnO_4$ modification, Environ. Sci. Pollut. Res. 26 (2019) 8902–8913.
[26] L. Huang, J. Kong, W. Wang, C. Zhang, S. Niu, B. Gao, Study on Fe(III) and Mn(II) modified activated carbons derived from *Zizania latifolia* to removal basic fuchsin, Desalination 286 (2012) 268–276.
[27] J. Chang, J. Ma, Q. Ma, D. Zhang, N. Qiao, M. Hu, H. Ma, Adsorption of methylene blue onto Fe_3O_4/activated montmorillonite nanocomposite, Appl. Clay Sci. 119 (2016) 132–140.
[28] M. Ghaedi, A. Ansari, F. Bahari, A.M. Ghaedi, A. Vafaei, A hybrid artificial neural network and particle swarm optimization for prediction of removal of hazardous dye brilliant green from aqueous solution using zinc sulfide nanoparticle loaded on activated carbon, Spectrochim. Acta, Part A 137 (2015) 1004–1015.
[29] S. Dashamiri, M. Ghaedi, K. Dashtian, M.R. Rahimi, A. Goudarzi, R. Jannesar, Ultrasonic enhancement of the simultaneous removal of quaternary toxic organic dyes by CuO nanoparticles loaded on activated carbon: central composite design, kinetic and isotherm study, Ultrason. Sonochem. 31 (2016) 546–557.
[30] P. Roy, N.K. Mondal, K. Das, Modeling of the adsorptive removal of arsenic: a statistical approach, J. Environ. Chem. Eng. 2 (2014) 585–597.
[31] S. Karnjanakom, P. Maneechakr, Adsorption behaviors and capacities of Cr(VI) onto environmentally activated carbon modified by cationic (HDTMA and DDAB) surfactants, J. Mol. Struct. 1186 (2019) 80–90.
[32] Y.S. Ho, G. McKay, Pseudo-second order model for sorption processes, Process Biochem. 34 (1999) 451–465.
[33] I.A.W. Tan, B.H. Hameed, A.L. Ahmad, Equilibrium and kinetic studies on basic dye adsorption by oil palm fibre activated carbon, Chem. Eng. J. 127 (2007) 111–119.
[34] A.V. Vitela-Rodriguez, J.R. Rangel-Mendez, Arsenic removal by modified activated carbons with iron hydro(oxide) nanoparticles, J. Environ. Manage. 114 (2013) 225–231.
[35] N. Li, Z. Mei, X. Wei, Study on sorption of chlorophenols from aqueous solutions by an insoluble copolymer containing β-cyclodextrin and polyamidoamine units, Chem. Eng. J. 192 (2012) 138–145.
[36] C.J. Hsu, H.J. Chiou, Y.H. Chen, K.S. Lin, M.J. Rood, H.C. His, Mercury adsorption and re-emission inhibition from actual WFGD wastewater using sulfur-containing activated carbon, Environ. Res. 168 (2019) 319–328.
[37] M.S. Karmacharya, V.K. Gupta, I. Tyagi, S. Agarwal, V.K. Jha, Removal of As(III) and As(V) using rubber tire derived activated carbon modified with alumina composite, J. Mol. Liq. 216 (2016) 836–844.
[38] H. Qi, S. Wang, H. Liu, Y. Gao, T. Wang, Y. Huang, Synthesis of an organic–inorganic polypyrrole/titanium(IV) biphosphate hybrid for Cr(VI) removal, J. Mol. Liq. 215 (2016) 402–409.
[39] J. Wu, D. Huang, X. Liu, J. Meng, C. Tang, J. Xu, Remediation of As(III) and Cd(II) co-contamination and its mechanism in aqueous systems by a novel calcium-based magnetic biochar, J. Hazard. Mater. 348 (2018) 10–19.
[40] D.H.K. Reddy, S.K. Lee, Magnetic biochar composite: facile synthesis, characterization, and application for heavy metal removal, Colloids Surf. A 454 (2014) 96–103.
[41] A.G. Karunanayake, O.A. Todd, M. Crowley, L. Ricchetti, Charles U. Pittman Jr., R. Anderson, D. Mohan, T. Mlsna, Lead and cadmium remediation using magnetized and nonmagnetized biochar from Douglas fir, Chem. Eng. J. 331 (2018) 480–491.
[42] D. Mohan, P. Singh, A. Sarswat, P.H. Steele, Charles U. Pittman Jr., Lead sorptive removal using magnetic and nonmagnetic fast pyrolysis energy cane biochars, J. Colloid Interface Sci. 448 (2015) 238–250.
[43] A.A. Edathil, I. Shittu, J. Hisham Zain, F. Banat, M.A. Haija, Novel magnetic coffee waste nanocomposite as effective bioadsorbent for Pb(II) removal from aqueous solutions, J. Environ. Chem. Eng. 6 (2018) 2390–2400.
[44] X. Guo, B. Du, Q. Wei, J. Yang, L. Hu, L. Yan, W. Xu, Synthesis of amino functionalized magnetic graphenes composite material and its application to remove Cr(VI), Pb(II), Hg(II), Cd(II) and Ni(II) from contaminated water, J. Hazard. Mater. 278 (2014) 211–220.
[45] N.M.M. Alvarez, J.M. Pastrana, Y. Lagos, J.J. Lozada, Evaluation of mercury (Hg^{2+}) adsorption capacity using exhausted coffee waste, Sustainable Chem. Pharm. 10 (2018) 60–70.
[46] T. Zhang, Y. Wang, Y. Kuang, R. Yang, J. Ma, S. Zhao, Y. Liao, H. Mao, Adsorptive removal of Cr^{3+} from aqueous solutions using chitosan microfibers immobilized with plant polyphenols as biosorbents with high capacity and selectivity, Appl. Surf. Sci. 404 (2017) 418–425.
[47] Z. Wu, R. Chen, Q. Gan, J. Li, T. Zhang, M. Ye, Mesoporous Na^+-SiO_2 spheres for efficient removal of Cr^{3+} from aqueous solution, J. Environ. Chem. Eng. 6 (2018) 1774–1782.